Experimental Astronomy
https://doi.org/10.1007/s10686-021-09820-x

ORIGINAL ARTICLE

Planetary polar explorer – the case for a next-generation remote sensing mission to low Mars orbit

Jürgen Oberst[1,2] · Kai Wickhusen[2] · Klaus Gwinner[2] · Ernst Hauber[2] · Alexander Stark[2] · Stephan Elgner[2] · Matthias Grott[2] · Lida Fanara[2] · Hauke Hussmann[2] · Gregor Steinbrügge[3] · Stephen Lewis[4] · Matthew Balme[4] · Maurizio Maugeri[5] · Guglielmina Diolaiuti[5] · Nanna Karlsson[6] · Andreas Johnsson[7] · Anton Ivanov[8] · Harald Hiesinger[9]

Received: 30 July 2020 / Accepted: 29 November 2021

Abstract

We propose the exploration of polar areas on Mars by a next-generation orbiter mission. In particular, we aim at studying the seasonal and regional variations in snow-deposits, which – in combination with measurements of temporal variations in rotation and gravity field – will improve models of the global planetary CO_2 cycle. A monitoring of polar scarps for rock falls and avalanche events may provide insights into the dynamics of ice sheets. The mapping of the complex layering of polar deposits, believed to contain an important record of climate history, may help us understand the early climate collapse on the planet. Hence, we propose an innovative next-generation exploration mission in polar circular Low Mars Orbit, which will be of interest to scientists and challenging to engineers alike. Schemes will be developed to overcome atmosphere drag forces acting upon the spacecraft by an electric propulsion system. Based on the experience of missions of similar type in Earth orbit we believe that a two-year mission in circular orbit is possible at altitudes as low as 150 km. Such a mission opens new opportunities for novel remote sensing approaches, not requiring excessive telescope equipment or power. We anticipate precision altimetry, powerful radars, high-resolution imaging, and magnetic field mapping.

Keywords Mars · Orbiter · Atmospheric drag · Electric propulsion · Altimetry · Radar

✉ Jürgen Oberst
Juergen.Oberst@dlr.de

Extended author information available on the last page of the article

Published online: 05 January 2022

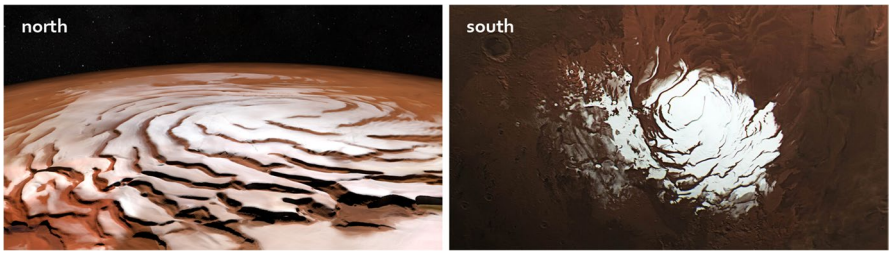

Fig. 1 Mars` polar caps as seen by the High Resolution Stereo Camera (HRSC) on ESA's Mars Express spacecraft. Credit: ESA/DLR/FU Berlin

1 Why study polar caps on Mars?

Owing to the presence of an atmosphere, ice reservoirs, and widespread evidence for past liquid water on its surface, Mars is the most Earth-like planet. While terrestrial climate change and its impact on the environment is of great concern to scientists and society alike, important lessons may be learned from studies of our neighbor planet.

Analysis of the Martian orbit and rotation reveal that the planet experienced notable variations in solar irradiation. There is ample evidence that Mars once had a dense atmosphere supporting liquid water bodies on the surface, which represented possible habitats for life forms at that time. Today, most of the atmosphere and water have vanished. Understanding this early climate collapse and identifying the current whereabouts of water on Mars are among the foremost issues in Solar System exploration and in research on the origin and evolution of life [32].

Telescope observations as early as those by Giovanni Domenico Cassini in 1666 revealed that Mars has pronounced polar caps (Fig. 1). Data from spacecraft orbiting Mars (starting with Mariner 9; [31] indicate that these are several kilometers thick and show layered structures, suggesting a complex sedimentation process of ice and dust (Fig. 2). Hence, these "polar layered deposits" (PLD) represent an important record for our understanding of the planet's climate history [3], 45. Currently, the polar caps play an important role in the Martian climate through an active exchange of volatiles with the atmosphere. Some of the most critical questions are: What are the physical characteristics of the PLDs and what record of climate change is expressed in their stratigraphy?

The appearance of the polar caps varies with season, owing to depositions (i.e., snow cover) and sublimation of large volumes of CO_2. This redistribution of CO_2 (involving almost one third of the total atmospheric CO_2) is associated with a planet-wide atmospheric circulation. The changing mass loads also cause measurable effects on Mars gravity and rotation. However, a full understanding of the dynamics of this scenario is still lacking.

The recent identification of a subglacial water lake by Mars Express adds to the intriguing nature of the polar caps and to prospects for exciting new discoveries in the future. Not surprisingly, a dedicated series of Mars Polar Science Conferences has periodically summarized our knowledge of the polar regions of Mars and

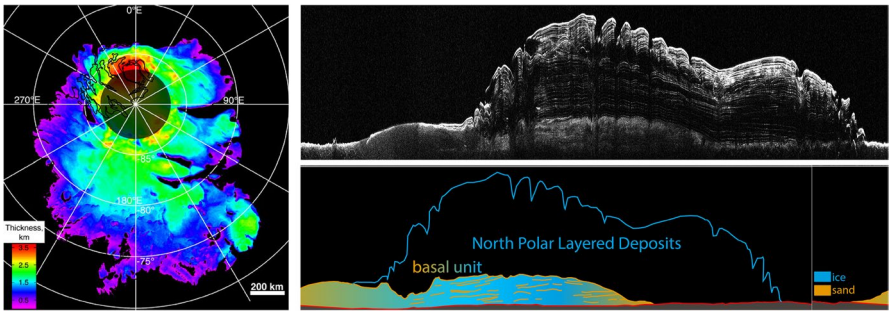

Fig. 2 Left: Thickness of south polar layered deposits of Mars, as probed by MARSIS on Mars Express. The dark contours outline the area of the residual summer ice cap. Image credit: NASA/JPL/ASI/ESA/ Univ. of Rome/MOLA Science Team/USGS; Right: Radar profile across the north polar deposits, acquired by the ground penetrating radar SHARAD on NASA's Mars Reconnaissance Orbiter. Credit: NASA/ASI/Nerozzi

identified key science questions that are critical to advance beyond the present stage [5–8, 14, 47]. Moreover, the study of the polar caps is mandatory to address fundamental science questions related to the recent and ongoing evolution of Mars volatiles and climate [29], 30. As a key future element to study the polar caps, essential for a better understanding and characterization of Mars polar areas, a next-generation remote sensing mission will be required.

2 Mars polar caps

The visual appearance, structure, and dynamics of Mars' North and South polar caps are complex – and they show puzzling differences. Both caps represent unique laboratories, useful for studies of other planetary polar environments, including the terrestrial Arctic and Antarctic.

North and South The North polar cap covers an area of approximately 1100 km in diameter, the Southern cap being significantly smaller (400 km). The caps are more than 2 - 3 kilometers thick in places (Fig. 2), consisting mostly of water ice with only a small component of dust, as data from the Mars Advanced Radar for Subsurface and Ionospheric Sounding (MARSIS) on Mars Express suggest (Fig. 2). The South polar caps, which are exposed to longer and colder winter seasons than their northern counterpart, are covered by additional (~10 m) CO_2 (dry ice).

The morphologies of both polar caps are complex and far from understood. At the margins, the caps rise gently; in other places, they are characterized by steep scarps. Spiral-shaped troughs on both polar caps (Fig. 1) are probably related to prevailing wind patterns associated with Mars' rotation and Coriolis forces.

Seasons Just like for Earth, the rotation axis of Mars is tilted with respect to its orbital plane, and the planet undergoes a seasonal cycle of changing Solar irradiation on the northern and southern hemisphere – leaving the polar areas in winter

darkness. Owing to the notable eccentricity of Mars' orbit, the orbital speed and the solar distance of the planet vary during the year, adding to the seasonal effect of changing irradiation levels. As a consequence, Southern winter seasons are particularly long and cold.

In addition to the permanent ice, the polar caps are covered by thin sheets of CO_2 ice in the winter season, which are sublimating during the spring. The overall statistics of data from the Mars Orbiting Laser Altimeter (MOLA) revealed the seasonal snow depth of Mars polar deposits at a maximum of 1.5 – 2 m. However, the precise areal distribution and local depths of the deposits are unknown. The effect implies a substantial redistribution of atmospheric CO_2 during the seasons, involving one third of the total atmospheric mass (3×10^{15} kg; [43]. The seasonal redistribution of these loads affects the moment of inertia of the planet body and causes measurable effects on Mars gravity (i.e., the gravitational flattening) and rotation (i.e., length of day variation). More precise measurements of this interaction between surface and atmosphere may help us improve the models of global mass transport and circulation of the atmosphere.

Layered Deposits Mars has experienced dramatic climate changes in the past. Numerical simulations of the coupling of Mars' spin and orbit reveal that obliquity and eccentricity varied substantially over comparably short time scales of 10 million years, causing changing solar irradiation and climate (Fig. 3, left). The seasonal deposition of ice and dust varied accordingly, leaving a record in the polar areas. Indeed, exposed walls of troughs and scarps in the polar caps show marked layers of deposits of dusty ice (see Fig. 3, right), which often can be traced over hundreds of kilometers. Surface textures and unconformities probably reflect physical properties of the layers (such as dust content or ice grain size). Periods where layers were eroded were followed by times when new layers were deposited. By studying the characteristics of the layers, we may understand how the Martian climate has changed, similar to how scientists on Earth study ice cores from the Arctic and Antarctic.

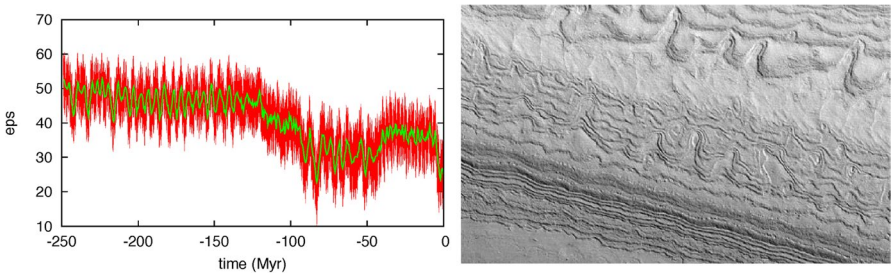

Fig. 3 Left: Mars' evolving obliquity (eps) in degree over time (red). The green curve denotes the obliquity when averaged over time intervals of 1 Myr. Right: Examples of polar layered deposits imaged by HiRISE onboard the Mars Reconnaissance Orbiter. Credit: NASA Jet Propulsion Laboratory

Subglacial water lakes? Orosei et al. [35] reported the detection of a subglacial lake beneath (~1.5 km) the southern polar ice cap, and spanning 20 km horizontally, as implied from a bright radar echo obtained by the MARSIS radar on Mars Express. While liquid water bodies cannot be sustained at the surface at the given temperature and pressure of the atmosphere, the survival of brines (saline waters) below the surface is conceivable.

Owing to limited data coverage of MARSIS, it is plausible that subsurface water may be found in other locations as well. Lake Vostok in Antarctica is a well-known terrestrial analog. The idea is most intriguing that such subglacial lakes, in spite of extreme environmental conditions, represent possible habitats for life forms.

Activity on polar scarps Most of the polar cap margins are characterized by steep scarps. The High Resolution Imaging Science Experiment (HiRISE) on-board the Mars Reconnaissance Orbiter monitored present activity along the scarps. Benefitting from its near-polar orbit, HiRISE has observed and revisited tens-of-kilometers-long scarps, where it revealed evidence for avalanches and block falls occurring [40, 41].

The ice cap margins are the first to lose the CO_2 snow layers that cover the PLD in winter and sublimate in spring [19, 37]. The diurnal temperature variations result in thermal stress-induced fracturing of both the lower part of the PLD and the underlying sandy Basal Unit (BU) leading to block falls [4]. This active mass wasting is thought to cause measurable scarp retreat [20].

The process competes with the gradual (~0.22-0.9 mm/yr) accumulation of dust on PLDs [36, 46, 48] and with viscous flow of the ice sheets [48], as is suggested by shape and slopes observed in local parts of the PLDs [24]. Consequently, accurate estimates of morphology of the ice caps and the erosion rates on scarps are a key to understanding which process controls the current evolution of scarps and the dynamics of the polar caps.

3 Limitations of current Mars data

Mars Gravity and Rotation The gravity field of Mars has been studied from radio science observations by spacecraft in orbit about the planet, including Mars Global Surveyor, Mars Odyssey, Mars Reconnaissance Orbiter, and Mars Express. Genova et al. [17] recently obtained a gravity field expressed in spherical harmonics to degree and order 120 (Goddard Mars Model 3, GMM-3), the quality of which, however, is not globally uniform. At the south pole the effective degree strength is about 100, while at the north pole it is only as high as 85 (Fig. 4).

The time variability of the gravity field, i.e., periodic variations due to solar and Phobos tides, atmospheric loads, and seasonal mass relocations from pole-to-pole, is of particular interest. Genova et al. [17] have considered annual, semi-annual, and tri-annual models for the zonal harmonics C_{20}, C_{30}, C_{40}, and C_{50}. However, clearly, at both poles of Mars the resolution of the gravity field is not sufficient to perform

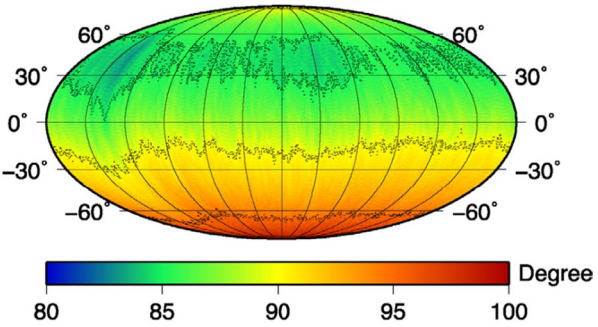

Fig. 4 Goddard Mars Model 3 (GMM-3) degree strength (Figure taken from: [17]

detailed analysis of the properties of ice caps. Gravity solutions by Zuber et al. [52], Konopliv et al. [27] and Genova et al. [17] suggested that lowlands within the north polar layered terrains do not correlate with gravity anomalies in these regions. This lack of correlation might be caused by heterogenous material in the lower crust or upper mantle, or mascons of sedimentary and/or volcanic depositions [17]. This enigma can be only solved by a detailed study of the gravity field anomalies at the poles in higher resolution.

The rotation of Mars was precisely measured by radio tracking of landers on the surface. Data from Mars Pathfinder revealed significant variations in the length of day as early as in 1997 [15]. Further continuous tracking of landers has revealed nutations related to the Martian seasonal cycle [26]. The InSight mission, currently operating on the Martian surface, is likely to detect nutations associated with the core of Mars [9], 16.

Mars altimetry The Mars Global Surveyor (MGS) was launched in November 1996, and began orbital mapping in March 1999. The onboard Mars Orbiter Laser Altimeter (MOLA) operated until June 2001 (i.e., for one Mars year). The instrument measured the time-of-flight of infrared Laser pulses towards Mars at a rate of 10 Hz to determine the range of the spacecraft to the surface. MOLA also functioned as a passive radiometer, and measured the radiance of the surface of Mars at 1064 nm. The vertical (shot-to-shot) precision was 37.5 cm; the absolute vertical accuracy (which depended on the accuracy of reconstruction of the spacecraft orbit) was $<$10 m. From the given orbit height and spacecraft speed, the Laser spot size on the surface was approximately 130 m; the along-track shot spacing was 330 m. MOLA successfully obtained more than 600 million data returns.

MOLA's range measurements have been used to construct a precise topographic map of Mars, an important reference data set up to the present day, with many applications to studies in geophysics, geology and atmospheric circulation. The map showed the full variety of terrain types on the Martian surface (Fig. 5) including e.g., the low northern hemisphere, the Tharsis province, Valles Marineris, the southern highlands and both polar caps. Measurements of topography also contributed to understanding the pathways of liquid water flowing on early Mars.

MOLA detected seasonal variations of snow deposits at the polar caps of 1.5 m to 2 m maximum during the Martian winter [43, 53] at an effective resolution of only

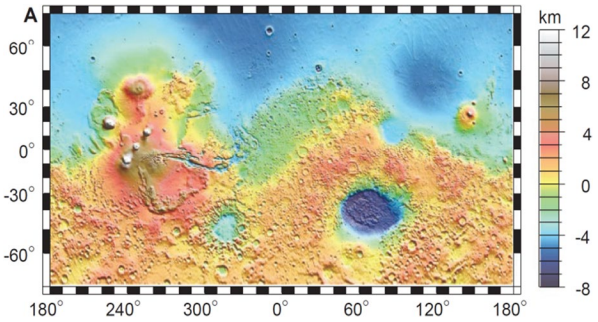

Fig. 5 Map of the global topography of Mars derived from MOLA (Mercator projection), featuring the Tharsis volcano-tectonic province (220°E to 300°E), which includes the Valles Marineris canyon system and several major volcanic shields: Olympus Mons, Alba Patera and others. The Hellas basin is located in the southern highlands. Figure modified from [52]

10 cm. MOLA also detected cloud structures in the planet's atmosphere. Clouds were identified that were reflective at the Laser wavelength of 1064 nm,others were opaque – absorbing the return pulse [33]. Formation and migration of the clouds could be tracked and interpreted with respect to the seasonal cycles on Mars.

Unfortunately, there was little information in the "shape" of returning Laser pulses, known to contain precious information on atmospheric structure, not to mention surface slopes and surface roughness. In the worst case (e.g., in ice-covered polar areas) shots were saturated and yielded shot arrival time only. Occasionally, cloud cover prevented the mapping of ground topography. As the orbit was not perfectly polar ($i \approx 93°$), areas at high latitudes could only be mapped by occasional tilting of the spacecraft, thus resulting in coverage gaps, as well as limited knowledge on instrument pointing, coordinates of the ground spot, and height accuracy.

Radar data Radar sounding is well established in planetary science, and the technique has been successfully applied to Mars. The Mars Advanced Radar for Subsurface and Ionosphere Sounding (MARSIS; [22] on board ESA's Mars Express mission mapped the thickness of the ice sheet (Fig. 2). MARSIS complemented by the SHAllow RADar sounder (SHARAD, [42] on board NASA's Mars Reconnaissance Orbiter (MRO, [54].

Unfortunately, owing to different characteristics of MARSIS and SHARAD in terms of frequency and power, signal attenuation and visibility of subsurface layering by the two instruments is quite different, the full reasons for this remaining unclear. Thus, the radar data leave significant ambiguities in a scientifically outstanding question. For example, the basal layer is poorly resolved, and can be traced with confidence only in the MARSIS data. Also, the reflector identified and interpreted as a subsurface lake [35] is only visible in MARSIS data.

Imaging data Owing to seasonal changes in illumination and low-Sun conditions, imaging of polar areas is far from trivial. While the polar regions are completely covered by images with scales of tens to hundreds of meters (e.g., [38], the

situation is different for image data sets with higher resolution. A mosaic based on CTX images with a scale of 5 m/pixel covers all of Mars from between 88°S and 88°N [10], thus missing some small parts of the polar caps. The availability of very high-resolution data from the HiRISE camera (25-30 cm/px) (see Fig. 6), however, is limited to about 2% of the Martian surface. While the repeat HiRISE imagery for change monitoring is locally very good (e.g., [13], many other areas expected to show seasonal and interannual changes are poorly covered. Additional images at scales of tens of cm and ultrahigh-resolution images at scales of ~5 cm/px [29] would dramatically enhance our ability to reveal stratigraphic details and thus the climate record stored in the polar layered deposits, and an even higher cadence of repeat imaging distributed over the entire Martian year (except when the polar caps are not illuminated in winter) at selected areas with a high potential for changes would enable a better understanding of the surface processes acting in this highly dynamic environment.

4 Next generation remote sensing mission

We propose a Next-Generation Remote Sensing (ESA M-Class) mission to Mars, involving a spacecraft in circular Low Mars Orbit (LMO) (< 150 km), supported by electric propulsion. Due to the atmospheric drag, spacecraft in circular orbits about the planet (e.g., MRO or the ExoMars Trace Gas Orbiter), typically orbit at altitudes of about 400 km. In contrast, Mars Express moves in a highly eccentric orbit, during which the spacecraft approaches the planet to within 250 km, however, only for short phases during the periapsis pass (e.g., [21].. Remote sensing can benefit from such a mission in LMO in terms of better data resolution, while sounding instruments may profit from high signal strength. We anticipate high-resolution imaging (not requiring excessive telescope equipment), as well as radar sounding and Laser altimetry (not requiring excessive power). Magnetic field mapping will enjoy high signal strength and high spatial resolution of data.

We may carry out a quick back-of-the envelope analysis for atmospheric friction to be anticipated and its compensation. The thin atmosphere of Mars and the

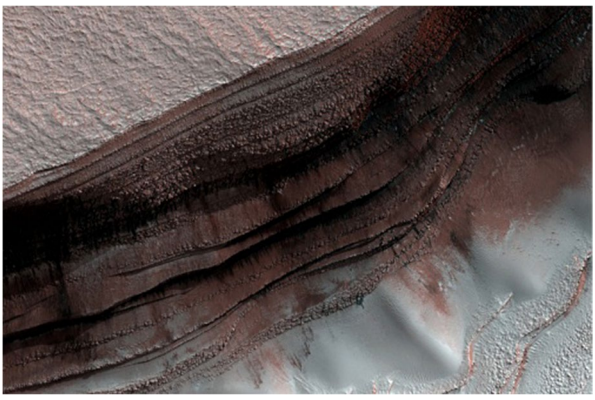

Fig. 6 Example of HiRISE image of PLDs (cf. also: Figure 3). Credit: NASA Jet Propulsion Laboratory

resulting drag reduces the altitude of a spacecraft. In order to avoid a de-orbiting of the spacecraft we use an electric propulsion system which compensates the drag force. We consider a simple scale height model, which yields Mars' atmospheric density for given spacecraft height h of the type:

$$\rho(h) = \rho_0 * e^{-h/H}$$

with ρ_0 being the reference density at the reference surface (0.001 kg/m^3 < ρ_0 < 0.0001 kg/m^3) and H is the atmospheric scale height (11.1 km). We also may consider explicit models of the Martian atmosphere, which is known to vary with latitude, with time of day and season (e.g., The Mars Climate Database, MCD v 5.3 [http://www-mars.lmd.jussieu.fr/mars/access.html]). To determine the drag force, which acts on the spacecraft, we may use:

$$F(h) = {}^{1}\!/_{2}\,\rho(h)v(h)^2 C_D A$$

where A is spacecraft cross section, v(h) is spacecraft velocity (for LMO: 3.45-3.55 km/s) and C_D is the drag coefficient (typical dimensionless number: 2.0).

We assume a spacecraft cross section of 10 m^2 to determine the resulting drag force to be compensated by electric propulsion. For example, the BepiColombo transfer module is equipped with two thrusters, at a thrust of up to 125 mN, each. The DAWN spacecraft is equipped with three engines, each of which delivers a thrust of 90 mN. We determined at which distance the electrical propulsion system would be capable to compensate the atmospheric drag. As a result, we find that stable orbits at an altitude of 150 km can comfortably be achieved and sustained for a mission of 1-2 Mars years.

The proposed mission relies on important ESA heritage: The GOCE (Gravity field and steady-state Ocean Circulation Explorer) was launched in 2009, to map the Earth's gravity field at unprecedented details at that time. The satellite's unique

Fig. 7 GOCE spacecraft, artist's conception. Credit: ESA - AOES Medialab; GFZ

arrow shape and fins (Fig. 7) helped keep GOCE stable as it flew through the upper atmosphere at a comparatively low altitude of 255 kilometers. An ion propulsion system compensated for the variable deceleration due to air drag. The spacecraft's primary instrumentation was a highly sensitive gravity gradiometer. After running out of propellant, the satellite made an uncontrolled atmospheric reentry on 11 November 2013.

We expect that the proposed mission can be realized within the M-class as defined by ESA. It has to overcome a number of challenges.

(1) We must optimize the spacecraft shape, to minimize drag. Just like in the case of GOCE, winglets may be used to support attitude control of the craft and possibly even to provide some lift.
(2) We must optimize the orbit to warrant access to solar power, required to support electric propulsion. We may study Sun-synchronous orbits, in particular the terminator orbit. As in this case the Sun position vector is perpendicular to the spacecraft motion vector, the drag force acting upon the solar panels is minimized.
(3) We must consider Mars' atmospheric structure and its temporal/spatial variations. In particular, dust storms may pose a challenge to the mission, as atmospheric density increases dramatically during such events and may require the spacecraft to move temporarily into a higher orbit.

5 Instruments

Radio science We aim at a refinement of Mars' gravity field. Here, radio tracking of the spacecraft using state-of-the-art radio science equipment (e.g., USO) is critical. We aim at recovering gravity field parameters of degree and order > 200. Specifically, we aim at measurements of time-varying effects of the field (notably, the variation of zonal harmonics), representing atmospheric circulation and the seasonal mass re-distribution.

The drag of the atmosphere adds substantial non-gravitational perturbation to the spacecraft orbit. Hence, this drag must be measured by an accelerometer to allow the correction of this effect. The BepiColombo spacecraft, where radio science is combined with observations of spacecraft motion by an accelerometer may be a good example. Measurements of the spacecraft drag may be used for studies of Mars' atmospheric density structure.

Next generation laser altimeter and atmospheric lidar While data from MOLA are now more than 20 years old (data acquisition began in March 1999 and lasted until June 30, 2001), a Next Generation Laser Altimeter should focus on seasonal changes for understanding the climate cycles on Mars. The measurements should include precise determination of height variations of the polar caps for at least two Martian years. Volumes of seasonal deposits and rates of sublimation of snow in polar areas

shall be determined for improving the models of the global CO_2 cycle. This shall be accompanied by measurements of wind speed and tracking of clouds. Studying the Martian atmosphere, cloud heights, opacity of the Martian atmosphere and the vertical distribution of dust, in particular, during dust storms shall be measured.

These diverse scientific objectives require a flexible Laser system, suitable for both precise range measurements to the ground as well as atmospheric sounding, including precise measurements of attenuation and reflectivity in the atmosphere. A Laser altimeter suitable for the described tasks could be based on LOLA (Lunar Orbiting Laser Altimeter; [44] or the ICESat-2 Laser altimeter ATLAS (Advanced Topographical Laser Altimeter System). We propose a high (order of kHz) shot rate and multiple parallel altimeter tracks from one orbit pass (Fig. 8), using a beam splitter [28]. The typical pulse width is on the order of several ns and the pulse energy is around 1 mJ per shot, thus requiring a single-photon detection scheme. Shot statistics will be used to measure surface albedo, roughness, and atmospheric structure parameters. The system shall operate at multiple Laser wavelengths to support atmospheric sounding. While 1064 nm and 532 nm are typical for ranging tasks and geodetic applications, the Laser light at a wavelength of 2.1 µm and 1.6 µm is known to be sensitive for CO_2 absorptions. However, the appropriate Lasers are yet to be flown in space applications.

Newly developed onboard noise cancellation techniques improving signal detection and range acquisition can be expected for this kind of development [1]. The main ground data processing tasks include the formation of super-resolution gridded topographic models, benefitting from multiple overlap of Laser spots, Laser cross-track analysis (or self-registration, [49] to solve for spacecraft orbit corrections and Mars rotation model parameters. The instrument will benefit very much from the low orbit height, resulting in smaller ground footprint size and higher return signal strength.

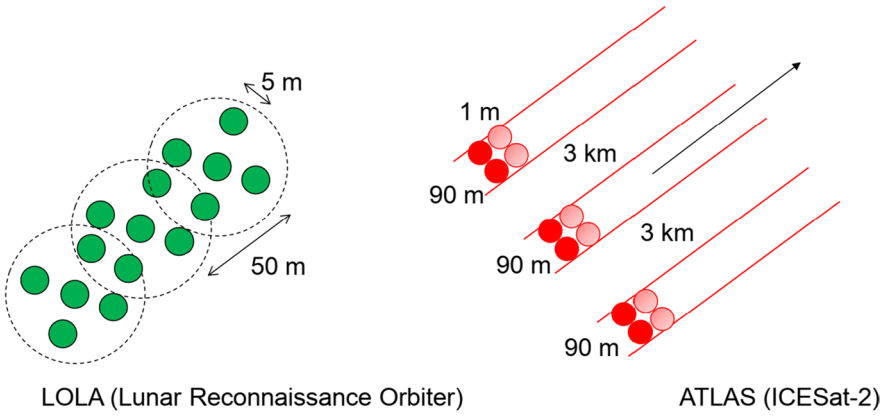

Fig. 8 Multi-beam patterns of the LOLA and ATLAS instruments on board LRO and ICESat-2, respectively

Imaging Experiment Multi-temporal mapping of polar scarps shall be carried out to study dynamics of ice sheets and to identify time-varying features, such as rock falls and avalanche events. Modern machine-learning and change detection methods are an important key for the analysis of the image data.

Radar The past decades of planetary exploration relied significantly on space-borne radars to explore the subsurface of moons and comets [18, 23, 25, 39]. Prominent examples are the Lunar Radar Sounder (LRS, [34] on-board the Selenological and Engineering Explorer (SELENE) spacecraft and the Comet Nucleus Sounding Experiment by Radiowave Transmission (CONSERT) instrument [25] as part of the Rosetta mission.

Radars on a future Mars Remote Sensing mission will require a versatile instrument, as demonstrated by RADAR [11] on board the Cassini mission, which combined the functionality of an imaging radar (e.g., [12] and an altimeter (e.g., [51]. By using multiple frequencies, as foreseen for the Radar for Europa Assessment and Sounding: Ocean to Near-surface (REASON), we will be able to characterize the subsurface mechanical and thermal structure, to probe surface composition [2], and support altimetry [50]. Such a radar allows deeper insights into the extent and structure of the Martian polar deposits to be obtained. Searching for reflectors from putative subsurface lakes at appropriate frequencies allowing for better resolution would be among the primary goals of a future instrument to characterize the abundance of subsurface water on Mars. Orbiter concepts involving lower altitudes would allow for better signal-to-noise ratios hence permitting higher frequencies at similar penetration depth or deeper penetration for continuing the search for Martian aquifers.

6 Conclusion

For the next-generation exploration of Mars, we propose dedicated studies of the polar caps, which are critical for our understanding of global atmospheric circulation and contain critical information on the climate record of the planet. This may be carried out by a new M-class remote sensing mission in a polar Low Mars Orbit (< 150 km), the spacecraft being equipped with next-generation onboard instruments, e.g., multi-beam Laser altimeters, a powerful sounding radar and high-resolution imaging experiments (Fig. 9). Such a mission may support our understanding of the early climate collapse on Mars, the whereabouts of water, and may even support the understanding of climate change on Earth.

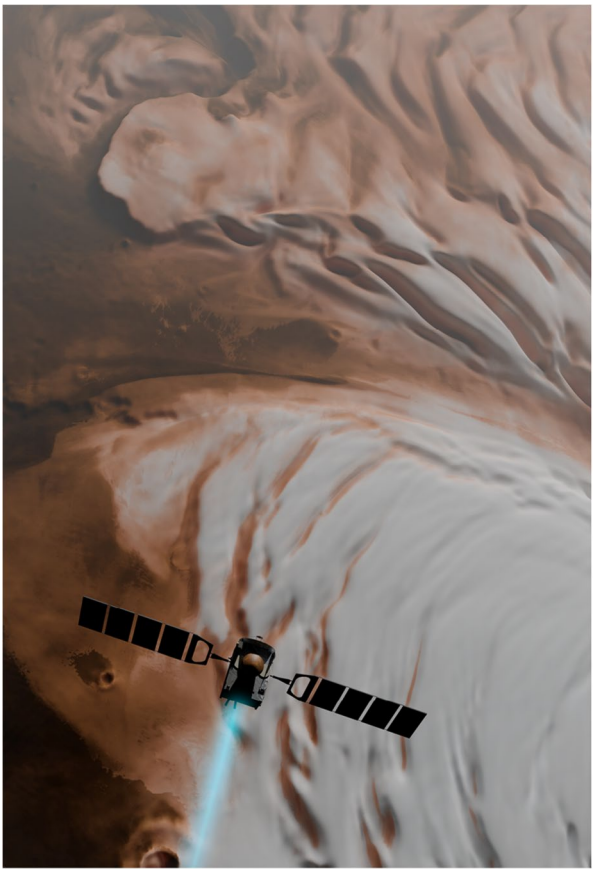

Fig. 9 Mars Polar Orbiter, artist's view. Background image: HRSC image of Chasma Boreale. Credit: ESA/DLR/FU Berlin

Funding Open Access funding enabled and organized by Projekt DEAL.

Declarations

Conflict of interest No funding was received to assist with the preparation of this manuscript.

References

1. Bae, S., Webb, C.E.: Precision attitude determination with an extended kalman filter to measure ice-sheet elevation. J. Guid. Control Dyn. **40**, 2335–2340 (2017)
2. Blankenship, D.D., Young, D.A., Moore, W.B., Moore, J.C.: Radar Sounding of Europa's Subsurface Properties and Processes: The View from Earth. In: Pappalardo, R.T., McKinnon, W.B., Khurana, K.K. (eds.) Europa, pp. 631–654. The University of Arizona Press, Tuscon (2009)
3. Byrne, S.: The polar deposits of Mars. Annu. Rev. Earth Planet. Sci. **37**, 535–60 (2009). https://doi.org/10.1146/annurev.earth.031208.100101
4. Byrne, S., Sori, M. M., Russell, P., Pathare, A. V., Becerra, P., Molaro, J. L., Sutton, S., Mellon, M. T., HiRISE Team: Mars polar cliffs: stressed out and falling apart. European Planetary Science Congress 11, EPSC Abstracts 11, EPSC2017-333 (2017)
5. Clifford, S.M., et al.: The state and future of Mars polar science and exploration. Icarus **144**, 210–242 (2000). https://doi.org/10.1006/icar.1999.6290
6. Clifford, S.M., Thosteinsson, Th., Björnsson, H., Fisher, D.A., Paige, D.A.: Introduction to the second Mars polar science special issue. Icarus **154**, 1–2 (2001). https://doi.org/10.1006/icar.2001.6727
7. Clifford, S.M., Doran, P.T., Fisher, D.A., Herd, C.D.K.: Third Mars polar science special issue: key questions, needed observations, and recommended investigations. Icarus **174**, 291–293 (2005). https://doi.org/10.1016/j.icarus.2004.12.012
8. Clifford, S.M., et al.: Introduction to the fifth Mars Polar Science special issue: key questions, needed observations, and recommended investigations. Icarus **225**, 864–868 (2013). https://doi.org/10.1016/j.icarus.2013.04.005
9. Dehant, V., Banerdt, B., Lognonne, P., Grott, M., Asmar, S., Biele, J., Breuer, D., Forget, F., Jaumann, R., Johnson, C., Knapmeyer, M., Langlais, B., Le Feuvre, M., Mimoun, D., Mocquet, A., Read, P., Rivoldini, A., Romberg, O., Schubert, G., Smrekar, S., Spohn, T., Tortora, P., Ulamec, S., Vennerstrom, S.: Future Mars geophysical observatories for understanding its internal structure, rotation, and evolution. Planet. Space Sci. **68**, 123–145 (2012)
10. Dickson, J. L., Kerber, L. A., Fassett, C. I., Ehlmann, B. L.: A global, blended CTX Mosaic of Mars with vectorized seam mapping: A new mosaicking pipeline using principles of non-destructive image editing. 49th Lunar and Planetary Science Conference, LPI Contribution No. 2083, 2480 (2018)
11. Elachi, C., Allison, M.D., Borgarelli, L., Encrenaz, P., Im, E., Janssen, M.A., Johnson, W.T.K., Kirk, R.L., Lorenz, R.D., Lunine, J.I., Muhleman, D.O., Ostro, S.J., Picardi, G., Posa, F., Rapley, C.G., Roth, L.E., Seu, R., Soderblom, L.A., Vetrella, S., Wall, S.D., Wood, C.A., Zebker, H.A.: Radar: the Cassini titan radar mapper. Space Sci. Rev. **115**, 71–110 (2004). https://doi.org/10.1007/s11214-004-1438-9
12. Elachi, C., Wall, S., Janssen, M., Stofan, E., Lopes, R., Kirk, R., Lorenz, R., Lunine, J., Paganelli, F., Soderblom, L., Wood, C., Wye, L., Zebker, H., Anderson, Y., Ostro, S., Allison, M., Boehmer, R., Callahan, P., Encrenaz, P., Flamini, E., Francescetti, G., Gim, Y., Hamilton, G., Hensley, S., Johnson, W., Kelleher, K., Muhleman, D., Picardi, G., Posa, F., Roth, L., Seu, R., Shaer, S., Stiles, B., Vetrella, S., West, R.: Titan radar mapper observations from Cassini's T3 fly-by. Nature **441**, 709–713 (2006). https://doi.org/10.1038/nature04786
13. Fanara, L., Gwinner, K., Hauber, E., Oberst, J.: Present-day erosion rate of north polar scarps on Mars due to active mass wasting. Icarus **342**, article id. 113434 (2019). https://doi.org/10.1016/j.icarus.2019.113434
14. Fishbaugh, K.E., et al.: Introduction to the 4th Mars polar science and exploration conference special issue: five top questions in Mars polar science. Icarus **196**, 305–317 (2008). https://doi.org/10.1016/j.icarus.2008.05.001
15. Folkner, W.M., Yoder, C.F., Yuan, D.N., Standish, E.M., Preston, R.A.: Interior structure and seasonal mass redistribution of Mars from radio tracking of Mars Pathfinder. Science **278**, 1749–1752 (1997)
16. Folkner, W.M., Dehant, V., Le Maistre, S., Yseboodt, M., Rivoldini, A., Van Hoolst, T., Asmar, S.W., Golombek, M.P.: The rotation and interior structure experiment on the inSight mission to Mars. Space Sci. Rev. **214**, 100 (2018)
17. Genova, A., Goossens, S., Lemoine, F.G., Mazarico, E., Neumann, G.A., Smith, D.E., Zuber, M.T.: Seasonal and static gravity field of Mars from MGS, Mars Odyssey and MRO radio science. Icarus **272**, 228–245 (2016)

18. Grima, C., Kofman, W., Herique, A., Orosei, R., Seu, R.: Quantitative analysis of Mars surface radar reflectivity at 20MHz. Icarus **220**, 84–99 (2012). https://doi.org/10.1016/j.icarus.2012.04.017
19. Hansen, C.J., Byrne, S., Portyankina, G., Bourke, M., Dundas, C., McEwen, A., Mellon, M., Pommerol, A., Thomas, N.: Observations of the northern seasonal polar cap on Mars: I Spring sublimation activity and processes. Icarus **225**, 881–897 (2013). https://doi.org/10.1016/j.icarus.2012.09.024
20. Herkenhoff, K.E., Byrne, S., Russell, P.S., Fishbaugh, K.E., McEwen, A.S.: Meter-scale morphology of the North Polar region of Mars. Science **317**, 1711–1715 (2007). https://doi.org/10.1126/science.1143544
21. Jaumann, R., et al.: The high-resolution stereo camera (HRSC) experiment on Mars express: instrument aspects and experiment conduct from interplanetary cruise through the nominal mission. Planet. Space Sci. **55**(7–8), 928–952 (2007). https://doi.org/10.1016/j.pss.2006.12.003
22. Jordan, R., Picardi, G., Plaut, J., Wheeler, K., Kirchner, D., Safaeinili, A., Johnson, W., Seu, R., Calabrese, D., Zampolini, E., Cicchetti, A., Huff, R., Gurnett, D., Ivanov, A., Kofman, W., Orosei, R., Thompson, T., Edenhofer, P., Bombaci, O.: The Mars Express MARSIS sounder instrument. Planet. Space Sci. **57**, 1975–1986 (2009). https://doi.org/10.1016/j.pss.2009.09.016
23. Kaku, T., Haruyama, J., Miyake, W., Kumamoto, A., Ishiyama, K., Nishibori, T., Yamamoto, K., Crites, S.T., Michikami, T., Yokota, Y., Sood, R., Melosh, H.J., Chappaz, L., Howell, K.C.: Detection of intact lava tubes at Marius hills on the moon by SELENE (Kaguya) lunar radar sounder. Geophys. Res. Lett. **44**, 10155–10161 (2017). https://doi.org/10.1002/2017GL074998
24. Karlsson, N.B., Holt, J.W., Hindmarsh, R.C.A.: Testing for flow in the north polar layered deposits of Mars using radar stratigraphy and a simple 3D ice-flow model. Geophys. Res. Lett. **38**, L24202 (2011). https://doi.org/10.1029/2011GL049630
25. Kofman, W., Herique, A., Barbin, Y., Barriot, J.P., Ciarletti, V., Clifford, S., Edenhofer, P., Elachi, C., Eyraud, C., Goutail, J.P., Heggy, E., Jorda, L., Lasue, J., Levasseur-Regourd, A.C., Nielsen, E., Pasquero, P., Preusker, F., Puget, P., Plettemeier, D., Rogez, Y., Sierks, H., Statz, C., Svedhem, H., Williams, I., Zine, S., Van Zyl, J.: Properties of the 67P/Churyumov-Gerasimenko interior revealed by CONSERT radar. Science (80) **349**, 1–7 (2015). https://doi.org/10.1126/science.aab0639
26. Konopliv, A.S., Park, R.S., Folkner, W.M.; An improved JPL Mars gravity field and orientation from Mars orbiter and lander tracking data. Icarus **274,** 253–260 (2016)
27. Konopliv, A.S., Yoder, C.F., Standish, E.M., Yuan, D.N., Sjogren, W.L.: A global solution for the Mars static and seasonal gravity, Mars orientation, phobos and deimos masses, and Mars ephemeris. Icarus **182**, 23–50 (2006)
28. Markus, T., et al.: The ice, cloud, and land elevation satellite-2 (ICESat-2): science requirements, concept, and implementation. Remote Sens. Environ. **190**, 260–273 (2017). https://doi.org/10.1016/j.rse.2016.12.029
29. MEPAG NEX-SAG Report. Report from the Next Orbiter Science Analysis Group (NEX-SAG), Chaired by B. Campbell and R. Zurek, 77 pages posted December, 2015 by the Mars Exploration Program Analysis Group (MEPAG) at https://mepag.jpl.nasa.gov/reports.cfm (2015). Accessed Jan 2022
30. MEPAG ICE-SAG Final Report. Report from the Ice and Climate Evolution Science Analysis group (ICE-SAG), Chaired by S. Diniega and N. E. Putzig, 157 pages posted 08 July 2019, by the Mars Exploration Program Analysis Group (MEPAG) at https://mepag.jpl.nasa.gov/reports.cfm (2019). Accessed Jan 2022
31. Murray, B.C., Soderblom, L.A., Cutts, J.A., Sharp, R.P., Milton, D.J., Leighton, R.B.: Geological framework of the south polar region ofMars. Icarus **17**, 328–345 (1972). https://doi.org/10.1016/0019-1035(72)90004-8
32. National Research Council. Vision and Voyages for Planetary Science in the Decade 2013-2022. The National Academies Press, Washington (2011). https://doi.org/10.17226/13117.
33. Neumann, G.A., Smith, D.E., Zuber, M.T.: Two years of clouds detected by the Mars orbiter laser altimeter. J. Geophys. Res. **108**(E4), 5023 (2003)
34. Ono, T., Oya, H.: Lunar Radar Sounder (LRS) experiment on-board the SELENE spacecraft. Earth Planets Sp. **52**, 629–637 (2000). https://doi.org/10.1186/BF03351671
35. Orosei, R., Lauro, S.E., Pettinelli, E., Cicchetti, A., Coradini, M., Cosciotti, B., Di Paolo, F., Flamini, E., Mattei, E., Pajola, M., Soldovieri, F., Cartacci, M., Cassenti, F., Frigeri, A., Giuppi, S., Martufi, R., Masdea, A., Mitri, G., Nenna, C., Noschese, R., Restano, M., Seu, R.: Radar evidence

of subglacial liquid water on Mars. Science **361**(6401), 490–493 (2018). https://doi.org/10.1126/science.aar7268
36. Perron, J.T., Huybers, P.: Is there an orbital signal in the polar layered deposits on Mars? Geology **37**(2), 155–158 (2009). https://doi.org/10.1130/G25143A.1
37. Piqueux, S., Kleinböhl, A., Hayne, P.O., Kass, D.M., Schofield, J.T., McCleese, D.J.: Variability of the martian seasonal CO2 cap extent over eight Mars years. Icarus **251**, 164–180 (2015). https://doi.org/10.1016/j.icarus.2014.10.045
38. Putri, A.R.D., Sidiropoulos, P., Jan-PeterMuller, J.-P., Walter, S.H.G., Michael, G.G.: A new south polar digital terrain model of Mars from the High-Resolution Stereo Camera (HRSC) onboard the ESA Mars express. Planet. Space Sci. **174**, 43–55 (2019). https://doi.org/10.1016/j.pss.2019.02.010
39. Putzig, N.E., Smith, I.B., Perry, M.R., Foss, F.J., Campbell, B.A., Phillips, R.J., Seu, R.: Three-dimensional radar imaging of structures and craters in the Martian polar caps. Icarus **308**, 138–147 (2018). https://doi.org/10.1016/j.icarus.2017.09.023
40. Russell, P., Thomas, N., Byrne, S., Herkenhoff, K., Fishbaugh, K., Bridges, N., Okubo, C., Milazzo, M., Daubar, I., Hansen, C., McEwen, A.: Seasonally active frost-dust avalanches on a north polar scarp of Mars captured by HiRISE. Geophys. Res. Lett. **35** (2008). https://doi.org/10.1029/2008GL035790
41. Russell, P.S., Byrne, S., Pathare, A., Herkenhoff, K.E.: Active erosion and evolution of Mars north polar scarps. 43rd Lunar and Planetary Science Conference, LPI Contribution No. 1659, 2747 (2012)
42. Seu, R., Biccari, D., Orosei, R., Lorenzoni, L.V., Phillips, R.J., Marinangeli, L., Picardi, G., Masdea, A., Zampolini, E.: SHARAD: The MRO 2005 shallow radar. Planet. Space Sci. **52**, 157–166 (2004). https://doi.org/10.1016/j.pss.2003.08.024
43. Smith, D.E., Zuber, M.T., Neumann, G.A.: Seasonal variations of snow depth on Mars. Science **294**, 2141–2146 (2001)
44. Smith, D.E., et al.: The Lunar Orbiter Laser Altimeter investigation on the Lunar Reconnaissance Orbiter Mission. Space Sci. Rev. **150**, 209–241 (2010). https://doi.org/10.1007/s11214-009-9512-y
45. Smith, I. B.: Mars Polar, Ice, and Climate Science: A Summary of Recent Work and our Current State of Knowledge. Ninth International Conference on Mars 2019 (LPI Contrib. No. 2089), 6306 (2019)
46. Smith, I.B., Putzig, N.E., Holt, J.W., Phillips, R.J.: An ice age recorded in the polar deposits on Mars. Science **352**(6289), 1075–1078 (2016). https://doi.org/10.1126/science.aad6968
47. Smith, I.B., et al.: 6th international conference on Mars polar science and exploration: conference summary and five top questions. Icarus **308**, 2–14 (2018). https://doi.org/10.1016/j.icarus.2017.06.027
48. Sori, M.M., Byrne, S., Hamilton, C.W., Landis, M.E.: Viscous flow rates of icy topography on the north polar layered deposits of Mars. Geophys. Res. Lett. **43**, 541–549 (2016). https://doi.org/10.1002/2015GL067298
49. Stark, A., Matz K.-D., Roatsch T.: Multi-Mission Laser Altimeter Data Processing and Co-Registration of Image and Laser Data at DLR, Planetary Science Informatics and Data Analytics Conference, held 24-26 April, 2018 in St. Louis, Missouri. LPI Contribution No. 2081, id.6014, 2018
50. Steinbrügge, G., Schroeder, D.M., Haynes, M.S., Hussmann, H., Grima, C., Blankenship, D.D.: Assessing the potential for measuring Europa's tidal Love number h2 using radar sounder and topographic imager data. Earth Planet. Sci. Lett. **482**, 334–341 (2018). https://doi.org/10.1016/j.epsl.2017.11.028
51. Zebker, H.A., Gim, Y., Callahan, P., Hensley, S., Lorenz, R.: Cassini radar team, analysis and interpretation of Cassini Titan radar altimeter echoes. Icarus **200**, 240–255 (2009). https://doi.org/10.1016/j.icarus.2008.10.023
52. Zuber, M.T., et al.: Internal structure and early thermal evolution of Mars from Mars Global Surveyor topography and gravity. Science **287**, 1788–1793 (2000)
53. Zuber, M.T., Phillips, R.J., Andrews-Hanna, J.C., Asmar, S.W., Konopliv, A.S., Lemoine, F.G., Plaut, J.J., Smith, D.E., Smrekar, S.E.: Density of Mars'south polar layered deposits. Science **317**, 1718–1719 (2007). https://doi.org/10.1126/science.1146995
54. Zurek, R.W., Smrekar, S.E.: An overview of the Mars Reconnaissance Orbiter (MRO) science mission. J. Geophys. Res. **112**, E05S01 (2007). https://doi.org/10.1029/2006JE002701

Authors and Affiliations

Jürgen Oberst[1,2] · Kai Wickhusen[2] · Klaus Gwinner[2] · Ernst Hauber[2] · Alexander Stark[2] · Stephan Elgner[2] · Matthias Grott[2] · Lida Fanara[2] · Hauke Hussmann[2] · Gregor Steinbrügge[3] · Stephen Lewis[4] · Matthew Balme[4] · Maurizio Maugeri[5] · Guglielmina Diolaiuti[5] · Nanna Karlsson[6] · Andreas Johnsson[7] · Anton Ivanov[8] · Harald Hiesinger[9]

[1] Technical University Berlin, Berlin, Germany

[2] DLR Institute of Planetary Research, Rutherfordstrasse 2, 12489 Berlin, Germany

[3] Institute for Geophysics, The University of Texas at Austin, Austin, TX, USA

[4] School of Physical Sciences, Open University, Milton Keynes, UK

[5] Department of Environmental Science and Policy, Università degli Studi di Milano, Milan, Italy

[6] Geological Survey of Denmark and Greenland, Copenhagen, Denmark

[7] Department of Earth Sciences, University of Gothenburg, Gothenburg, Sweden

[8] Space Center, Skolkovo Institute of Science and Technology, Moscow, Russia

[9] Institut für Planetologie, Westfälische Wilhelms-Universität (WWU), Münster, Germany